31st Annual International Conference of the IEEE EMBS
Minneapolis, Minnesota, USA, September 2-6, 2009

Measurement of the attenuation coefficient for monodisperse populations of ultrasound contrast agents

Yanjun Gong, Mario Cabodi, and Tyrone M. Porter, *Member IEEE*

***Abstract*—In this paper, we describe a technique for producing populations of ultrasound contrast agents (UCA) with a narrow size distribution. Using acoustic techniques, we measure the frequency-dependent attenuation coefficient for suspensions of ultrasound contrast agents with varying size distributions, ranging from narrow to wide. Our results demonstrate that as the size distribution becomes more uniform, attenuation occurs within a narrow frequency range. Additionally, as the mean size decreases, the peak in the attenuation coefficient occurs at a higher frequency.**

I. Introduction

Ultrasound has shown promise as an image modality for molecular imaging [1-9]. In this approach, ultrasound contrast agents (UCA) conjugated with a specific antibody are targeted to membrane-bound antigens that are expressed during the progression of a disease. Upon binding, diagnostic ultrasound images of the bound UCA are acquired and used in the evaluation of the anatomy and pathology of the disease. Ideally, UCA with the same frequency response would be used for molecular imaging applications. This would allow imaging to be conducted at frequencies tuned to the resonance or harmonics of the resonance of the bound bubbles, thus improving the sensitivity of the system for detecting the targeted UCA.

Recently, it has been shown that monodispersions of UCA can be produced using microfluidic devices [10-13]. In this study, we use similar techniques to produce narrowly distributed UCA and quantify the attenuation coefficient as a function of frequency and bubble size. From the experimentally-derived attenuation coefficient, we can determine the resonance frequency and compare with theoretical predictions.

II. Methods

A. Microfluidic Device

A flow focusing device was manufactured from polydimethylsioxane (PDMS) using photolithography techniques. There are four main microchannels in this device, one for gas inlet flow, two for liquid inlet flow, and the last one for microbubbles outlet flow (Figure 1). All the channels had a rectangular cross section with a height of 25μm. The widths of the liquid channel and gas channel were 50μm and 35μm, respectively, while the width of orifice was 7μm. A lipid solution and octafluoropropane were pushed through the liquid and gas channels, respectively. In the flow focusing chamber, the central stream of gas and two lateral streams of liquid merge and are forced through the 7-μm orifice. Microbubbles pinch off on the opposite side of the orifice, and by maintaining the liquid flow rate and gas pressure constant, it was possible to produce microbubbles with very narrow size distributions. The mean size of the microbubbles could be controlled by adjusting the gas pressure and liquid flow rate. The flow rate of the lipid solution was controlled with a syringe pump (KDS100, Fisher Scientific), while the octafluorpropane pressure within the gas channel was controlled with a pressure regulator. The size distribution of each batch of microbubbles was measured using a Coulter counter.

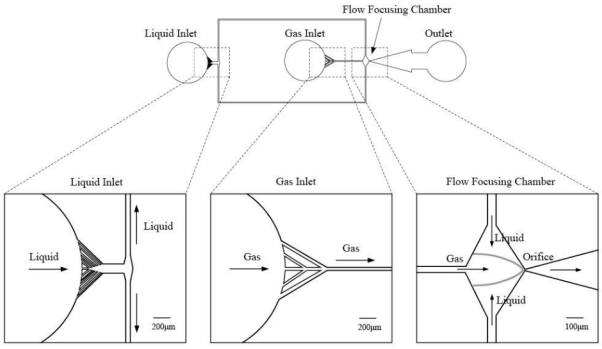

Figure 1. Schematic of the microfluidic device. A syringe pump was used to control the flow rate in the liquid channels, while a pressure regulator controlled the pressure in the gas channel. The liquid and gas converge in the flow focusing chamber and are forced through a narrow orifice, resulting in the formation of lipid-coated microbubbles.

B. Microbubble Composition

The microbubbles were made from a lipid solution and octafluoropropane. The lipid solution consisted of a mixture of DPPC (1,2-Dipalmitoyl-*sn*-Glycero-3-Phosphocholine, Avanti Polar Lipids), DPPA (1,2-Dipalmitoyl-*sn*-Glycero-3-Phosphate, Avanti Polar Lipids), and DPPE-PEG 5000 (1,2-Dipalmitoyl-*sn*-Glycero-3-Phosphoethanolamine-N-[Methoxy (polyethylene glycol)-5000], Avanti Polar Lipids) combined at a molar ratio of 81:8:10. The mixture was dissolved in chloroform ($CHCl_3$) and dried under argon overnight. The resultant film was further dried under vacuum to ensure removal of the organic solvent. The lipid film was rehydrated with saline, sonicated for 20 minutes in an ice bath, and the resultant vesicles were suspended in a

Y. Gong and T.M. Porter are with the Department of Mechanical Engineering, Boston University, Boston, MA 02215, USA. {ygong, tmp}@bu.edu

solution of 10% glycerol, 10% propylene glycol, and 80% deionized water.

C. Attenuation measurements

An ultrasound spectroscopy method [14] was used to measure the acoustic attenuation coefficient for UCA (Figure 2). The microbubble suspension was injected into an exposure chamber, which consisted of latex pulled over a plastic frame. The exposure chamber was submerged in a tank of degassed deionized water in front of a stainless steel (SS) plate, which served as a perfect reflector. Acoustic pulses were transmitted by a 2.25-MHz single element unfocused transducer, which was driven by a pulser/receiver (5072PR, Panametrics). Reflections from the UCA and SS plate were received by the transducer, amplified by the pulser/receiver, and digitized (f_s = 2.5 GHz) with a digital oscilloscope (Wavesurfer 64XS, LeCroy) before being saved on a desktop computer for frequency analysis. The attenuation coefficient was determined using the following equation:

$$\alpha_s = \alpha_w + \frac{1}{2d}\ln\left(\frac{|P_w(\omega)T(\omega)|}{|P_s(\omega)|}\right),$$

where a_w is the sound attenuation in water, $P_w(w)$ and $P_s(w)$ are the amplitude spectra of the chamber filled with water and microbubbles, respectively, $T(w)$ is the spectrum of the transmission coefficient across the medium-sample interface, and d is the thickness of the sample chamber. In this study, microbubbles with a narrow and broad size distribution (prepared via mechanical agitation) were tested, and the measured attenuation coefficients as a function of frequency were compared.

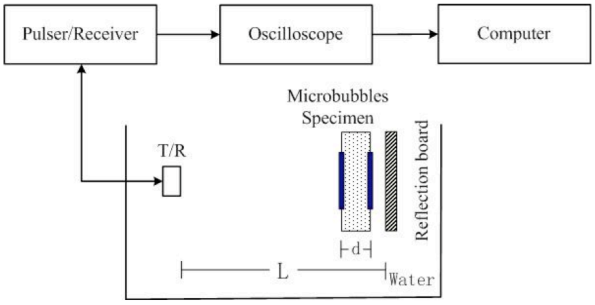

Figure 2. Schematic of experimental arrangement used for measuring frequency-dependent attenuation coefficient for ultrasound contrast agents.

III. Results

The size distribution for two batches of ultrasound contrast agents was measured with a Coulter counter. By precisely controlling the liquid flow rate and gas pressure, we successfully produced bubbles with mean diameters of 4.2±1 μm and 8±2 μm, respectively. The attenuation coefficients were measured for each population and compared with the attenuation coefficient measured for a suspension of polydisperse ultrasound contrast agents (Figure 3). As shown, the attenuation coefficients for the

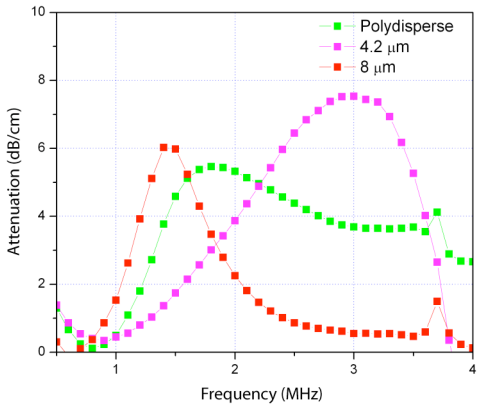

Figure 3. Attenuation coefficients for mono- and polydisperse ultrasound contrast agents (UCA). Attenuation for the monodisperse populations occurs over a more narrow bandwidth compared to the polydisperse population.

monodisperse suspensions peak at specific frequencies and have narrow bandwidths with local minima close to 0 dB/cm. The polydisperse population had measureable attenuation across a much wider bandwidth, peaking at 1.8 MHz. The attenuation coefficient within the bubble population is equal to the sum of the extinction cross-section for all of the suspended bubbles, which depends upon the radius and resonance frequency for each bubble, and the viscoelastic properties of the lipid shell. It is difficult to measure the viscoelastic properties (*i.e.* shell elasticity and viscosity) directly; however, it is possible to estimate these properties by measuring attenuation and scatter from UCA suspensions. The results reported in this study demonstrate the advantage of working with monodisperse populations of UCA. Additional studies will be conducted to quantify the attenuation and backscatter coefficients for monodispersions of UCA with varying mean diameters, and use this data to identify resonance frequencies and estimate viscoelastic properties of the shell. This approach can be used to design and characterize UCA, and select imaging frequencies that match the resonance of engineered UCA.

References

1. Bloch, S.H., P.A. Dayton, and K.W. Ferrara, *Targeted imaging using ultrasound contrast agents.* Ieee Engineering in Medicine and Biology Magazine, 2004. **23**(5): p. 18-29.
2. Dayton, P.A. and J.J. Rychak, *Molecular ultrasound imaging using microbubble contrast agents.* Frontiers in Bioscience, 2007. **12**: p. 5124-5142.
3. Hamilton, A., et al., *Left ventricular thrombus enhancement after intravenous injection of echogenic immunoliposomes - Studies in a new experimental model.* Circulation, 2002. **105**(23): p. 2772-2778.

4. Hamilton, A.J., et al., *Intravascular ultrasound molecular Imaging of atheroma components in vivo.* Journal of the American College of Cardiology, 2004. **43**(3): p. 453-460.
5. Klibanov, A.L., *Ultrasound molecular imaging with targeted microbubble contrast agents.* Journal of Nuclear Cardiology, 2007. **14**(6): p. 876-884.
6. Klibanov, A.L., et al., *Targeted ultrasound contrast agent for molecular imaging of inflammation in high-shear flow.* Contrast Media & Molecular Imaging, 2006. **1**(6): p. 259-266.
7. Leong-Poi, H., et al., *Noninvasive assessment of angiogenesis by ultrasound and microbubbles targeted to alpha(v)-integrins.* Circulation, 2003. **107**(3): p. 455-460.
8. Lindner, J.R., et al., *Noninvasive ultrasound imaging of inflammation using microbubbles targeted to activated leukocytes.* Circulation, 2000. **102**(22): p. 2745-2750.
9. Weller, G.E.R., et al., *Ultrasound contrast microbubbles targeted to ICAM-1 detect acute heart transplant rejection.* Circulation, 2002. **106**(19): p. 378-378.
10. Hettiarachchi, K., P. Dayton, and A.P. Lee, *Formulation of Monodisperse Contrast Agents in Microfluidics Systems for Ultrasound Imaging.* Proceedings of 2006 International Conference of Microtechnologies in medicine and Biology, 2006: p. 230-232.
11. Hettiarachchi, K., et al., *On-chip generation of microbubbles as a practical technology for manufacturing contrast agents for ultrasonic imaging.* Lab on a Chip, 2007. **7**(4): p. 463-468.
12. Talu, E., et al., *Maintaining monodispersity in a microbubble population formed by flow-focusing.* Langmuir, 2008. **24**(5): p. 1745-1749.
13. Talu, E., et al., *Tailoring the size distribution of ultrasound contrast agents: Possible method for improving sensitivity in molecular imaging.* Molecular Imaging, 2007. **6**(6): p. 384-392.
14. Hoff, L., P.C. Sontum, and J.M. Hovem, *Oscillations of polymeric microbubbles: Effect of the encapsulating shell.* Journal of the Acoustical Society of America, 2000. **107**(4): p. 2272-2280.